Measurement: Sensors 18 (2021) 100113

Contents lists available at ScienceDirect

Measurement: Sensors

journal homepage: www.sciencedirect.com/journal/measurement-sensors

Investigation on chromatic aberrations and its potential for application in depth measurement

ARTICLE INFO

Keywords
Chromatic aberrations
3D-reconstruction
Image processing

ABSTRACT

Chromatic aberrations are mostly supressed in typical industrial lenses to ensure a well-defined colour image. Beside the main wavelengths which are recognizable for the human eye, multispectral cameras can sample with a more detailed chromatic (spectral) resolution. This leads to a partial wavelength depended unsharpness in the images. If the imaging system can be well defined out of these imperfections, a depth information can be calculated. In this paper the theoretical model as well as a method for the 3D-reconstruction out of different colour (spectral) channels will be discussed.

1. Introduction

Optical systems consisting of one or more lenses are characterized by aberrations. The primary purpose of optical design and thus the preliminary work for camera lenses, vision and imaging systems is the fundamental reduction or even elimination of optical aberrations. This is achieved by an interplay of different lens designs consisting of a wide variety of materials.

Lenses are usually optimized to a certain point where only some errors are present to a sufficiently small degree. Only if an optic is almost perfectly free of aberrations it is suitable for precision measurement tasks.

One possibility is to use aberrations to realize certain measurement tasks. The chromatic aberration of the longitudinal error causes an axial offset of the wavelength dependent focal point as mentioned in the name [1]. Thus, it would be possible with a fixed sensor plane and different reference wavelengths to obtain sharp images of certain object distances. Depending on the object position, these focal planes can be shifted to the sensor and therefore a certain distance range of the object can be resolved and measured.

The aim of this work is to determine whether with a simple vision lens and a wavelength selection the effect of longitudinal chromatic aberration is present to an appropriate degree in order to subsequently perform length measurements in the object space with the evaluation of the sensor image. From the processed data, a 3D representation, i.e. the depth information of an object by means of passing through the chromatic areas, can be created.

2. Physical approach for estimating chromatic focal shift for depth measuring application

The longitudinal chromatic aberration is caused due to the dependence of the refractive index on the wavelength. In order to exploit this error for a depth measurement, it is important to understand how it occurs. It is best explained using a single bi-convex lens. In the field of geometrical optics, it can be assumed that a polychromatic and axis-parallel beam which runs outside the optical axis is chromatically split after passing through the lens and the individual colours are refracted differently. This collimated polychromatic light beam will experience different focal points in its spectral range. The focal length f(λ) increases with wavelength i.e. blue light has a shorter focal length than red light. The measurable distance of the focal points is also described as axial chromatic aberration [1].

$$D(\lambda) = \frac{1}{f(\lambda)} = (n(\lambda) - 1)\left(\frac{1}{R_1} - \frac{1}{R_2}\right) \tag{1}$$

Equation (1), the lens maker's formula, describes the refracting power D(λ) of the lens. It is calculated with the wavelength dependent refractive index n(λ) and with the radii of curvature R_1/R_2 of the lens surfaces. The reciprocal of the refracting power is the effective focal length f(λ) which is needed determine a focal point shift [2].

Fig. 1 explains the object distance shift with the help of geometrical optics. The upper drawing shows how the rear focal points and the image distance are affected by different wavelengths of a fixed object distance. The lower drawing takes the new wavelength depending focal points and displays the occurring object distance offset if the image plane stays in on place and the wavelength changes. This effect is the focal point shift caused by the longitudinal chromatic aberration.

To calculate an object distance g(λ) with the help of the focal point shift, the lens equation (2) (imaging equation) is used. By rearranging (2), the wavelength-dependent object distance of a lens can be determined (3). If (1) is now substituted into (3), an equation (4) is obtained which describes the object distance only as a function of the wavelength-dependent refractive index. The remaining parameters are given by the lens properties and the selected image distance b and are therefore constant in the equation. To calculate an object distance offset Δg(λ), a zero point is determined for the first object distance at an initial wavelength of $\lambda_0 = 330$ nm. The difference for the subsequent values is defined according to (5) over a specific wavelength range (λ_n). The object distance offset corresponds directly to the desired depth information of an image to be measured.

https://doi.org/10.1016/j.measen.2021.100113

Available online 20 September 2021

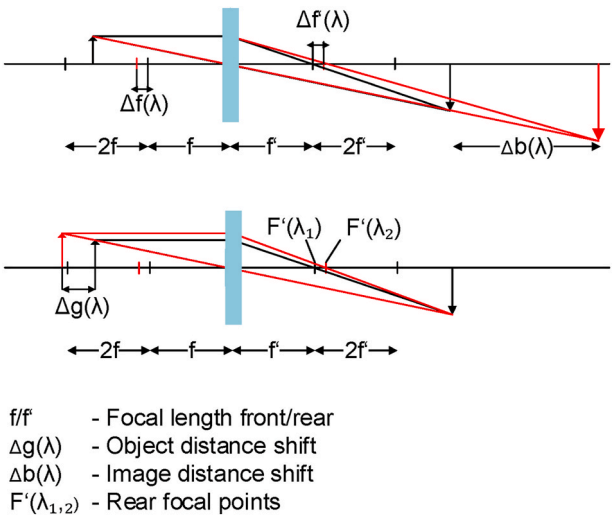

Fig. 1. Focal length depending on object distance.

$$\frac{1}{f(\lambda)} = \frac{1}{g} + \frac{1}{b} \tag{2}$$

$$\frac{1}{g(\lambda)} = \frac{1}{f(\lambda)} - \frac{1}{b} \tag{3}$$

$$g(\lambda) = \frac{R_2 R_1 b}{((R_2 - R_1)(n(\lambda) - 1))b - (R_2 R_1)} \tag{4}$$

$$\Delta g(\lambda) = g(\lambda_n) - g(\lambda_0) \tag{5}$$

It is now assumed that the imaging takes place at twice the focal length (magnification factor of 1). A single bi-convex lens made of N-BK7, with a focal length of 50 mm will therefore have an image distance of 100 mm. Fig. 2 displays the object distance offset and refractive index both dependent on the wavelength for the depicted lens [3].

In order to estimate how significant the error caused by a real lens is and to verify the calculated object distance offset, simulation models are created with the help of Zemax, an optical design and analysis software. A single bi-convex lens with the same parameters which are used in the calculation is evaluated. Later a comparison is made by experimental tests with the finished experimental setup of a multispectral image acquisition system.

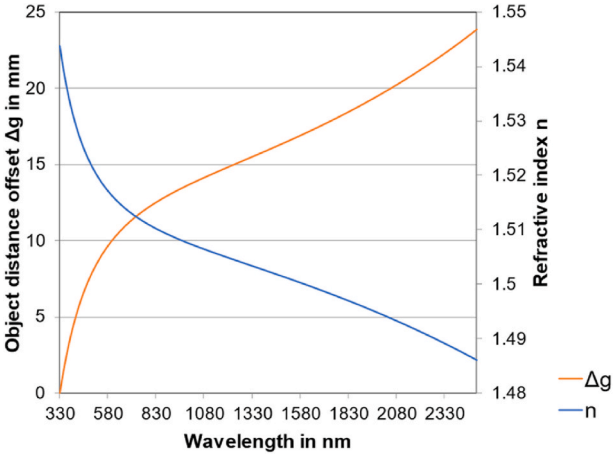

Fig. 2. Object distance offset and refractive index dependent on wavelength.

3. Numeric model of a convex lens and its chromatic focal shift

The depth measurement by means of longitudinal chromatic aberration is explained with an example in the form of a single bi-convex lens. The imaging of an object (inclined plane) is demonstrated with the help of Zemax. The simulation obtained by this method is then verified through experimental testing.

The chosen lens has a diameter of 25 mm and a focal length of 50 mm and is further used as an optical system with tubus and aperture in the simulation. The single lens shows as expected significant chromatic aberrations at an image distance of 100 mm. Table 1 shows the comparison of the calculated values with the simulation data of the example lens. Since the values of the numerical approach are approximately the same as those of the simulation, the lens can be tested in an experimental setup.

The simulation is performed in precise 1 nm steps from 400 nm to 950 nm, a focal shift and thus a depth information of about 9 mm can be measured, as shown in Fig. 3. For the experimental setup this is achieved with a multispectral camera and modulation of the light source in 1 nm steps.

It must be considered that for more complex vision systems, the currently present offset of the focal planes is not dependent on the position of the object in the object space. The chromatic aberration only shows the sharpness distribution (different focal planes) of the individual wavelengths in the image space. To evaluate the error correctly for the desired usability, the dependence in the object space must be added. The sensor is not shifted to the focal plane to enable a sharp image. The sensor remains at the same position and by changing the object distance through selecting the correct wavelength, a sharp image is obtained. The simulated system needs to be rotated (image and object space swapped) to obtain realistic results. However, a single bi-convex lens is used and therefore the object space has the same geometrical optical properties as the image space. If the different focal planes are now assumed as object distances, a clear dependence of the refractive index of the lens becomes apparent. The different focal planes have a larger focal length with a larger wavelength. This means that shorter object distances produce sharp images at lower wavelengths and larger object distances at longer wavelengths.

4. Method for determining the 3D-depth information

The numerically calculated object distances of an image can be converted to depth information by (5) as described in section 2. For the verification of a real system, consisting of the single bi-convex lens, a possibility is now introduced to convert the length information from the object distance into depth information with the help of a subsequent image processing.

For this purpose, a Matlab program was developed, which transfers focus information from 2D images into a 3D image. Fig. 4 describes the basic operation of the program.

To perform such an evaluation, it is necessary to record a series of images in the desired wavelength range. By modulating a light source, a spectrum with 1 nm bandwidth can be provided for each individual

Table 1
Comparison of focal shift of numeric approach and simulated data of an example single bi-convex lens.

Wavelength in nm	Focal shift in mm	
	Numeric	Simulated
400 (zero position)	0	0
500	3.53	3.55
600	5.56	5.58
700	6.88	6.9
800	7.83	7.85
900	8.59	8.58

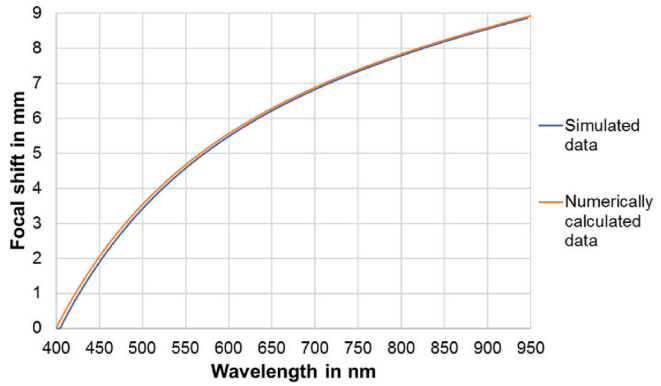

Fig. 3. Chromatic focal shift of the single bi-convex lens dependent of wavelength, numerical and simulated approach.

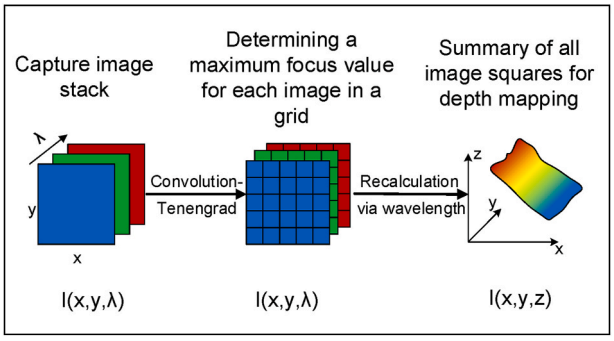

Fig. 4. Schematic course of image processing for the determination of depth information using only wavelength information.

image (left side, Fig. 4). According to the numerical approach, different object distances are also expected to have different focal planes. Each image therefore has a corresponding object distance for its wavelength. A loop is applied in which a parameterized mask is placed over the images as a square grid (middle, Fig. 4). For each square in the grid, a focus value is determined using a sharpness operator. The operator used here is the Tenengrad-Gradient (6) which convolutes the image with 3×3-Sobel-Operands s_x and s_y in both x and y orientations [4].

$$S = \sum_{(x,y)\in I} (I(x,y) * s_x)^2 + (I(x,y) * s_y)^2;$$

$$s_x = \begin{bmatrix} -1 & 0 & 1 \\ -2 & 0 & 2 \\ -1 & 0 & 1 \end{bmatrix}; \quad s_y = \begin{bmatrix} 1 & 2 & 1 \\ 0 & 0 & 0 \\ -1 & -2 & -1 \end{bmatrix} \tag{6}$$

These steps are repeated for the entire image stack. The focus values are then compared for each square in the grid. The maximum values for the respective image area are assembled as a new image (right side, Fig. 4). The newly composed image now consists of the sharpest planes of the individual wavelengths. By using the computation formulas (4) and (5), depth information can now be obtained from the image. The last step is a surface plot which maps the depth information as a 3D representation.

5. Experimental verification of the numeric approach

The numerically determined values of the lens are now being verified by means of an image evaluation. For this purpose, the image processing program which determines the focus values of individual image sections and compares them over their individual wavelengths, as described in section 4, is used.

The same type of single bi-convex lens as in the previous simulation was used to realize a test setup. It consists of a multispectral imaging system and the lens used as an objective. Single spectra of 1 nm bandwidth are generated with the help of a modulatable light source. An inclined plane was used as a test object. This was aligned in such a way that its depth information can be sufficiently represented over the sensor surface. This means in a 45° angle to the sensor surface. With the given dimension and a magnification factor of 1, a depth of 6 mm could be displayed. The intention is to confirm the numerical and simulated values of the focal shift. Since the depth information of the test object is known by the position of it, it is possible to obtain conclusions about the correctness of the measured values. Since the technical equipment does not allow a complete evaluation of the entire visible wavelength range, tests were performed in a wavelength range from 500 nm to 600 nm. For this purpose, as mentioned above, 101 images were acquired and evaluated in 1 nm steps. The result is shown in Fig. 5 and compared again with the numerical data in Table 2.

To compare the experimental data with the numerical ones, the geometric course of the inclined plane has to be defined. The measurable real depth of the plane can be determined with (7). This can be used because the mapping is performed with a magnification factor of 1.

$$\text{Depth inclined plane} = \frac{\text{Image Height}}{\tan(\alpha)}, \quad \alpha = 45\,^\circ \tag{7}$$

The lower edge of the image area corresponds to a depth of 0 mm because the image height is zero. For each image height, a depth can be calculated, which are both equal. This is justified because tan (45°) is equal to 1. In order to avoid further aberrations such as distortions, the effective measuring range was shifted to the centre of the image. The lower and upper flat areas in Fig. 5 show blurred planes. Due to the wavelength limitation, no reliable focus values could be determined at these locations. However, these errors do not affect the depth determination in the measurement area. The zero point for calculating the position of the inclined plane is therefore simply shifted in the image height to match the initial wavelength of 500 nm. In this way, reliable values can be obtained for the measurement range.

In Table 2, the experimentally determined depth and the numerical data are compared. The depth of the inclined plane is shown for the respective point at which the associated wavelength is most significant. For the single bi-convex lens the experimental data are approximately the same as the numerical for the respective wavelength.

The small deviation between the simulated depth of the plane and the experimental data can be explained by the angular error and stems from the simplified calculation. High-precision alignment was not possible, so there is a small error which still seems acceptable. This is because the image of the depth information represents the real system. This means that the error resides in (7) and not in the experimental data.

6. Conclusion and outlook

It was confirmed that with a single bi-convex lens it is possible to reconstruct a reliable 3D image out of different colour (spectral) channels by exploiting the longitudinal chromatic aberration. Since the concept was only proven, it is justifiable to state that structures in the millimetre range can be represented with this method. The measurement uncertainties were not determined and an exact resolution limit was not defined. It therefore has to be examined to what extent this approach can be applied.

The measurement resolution depends on the lens characteristics and can be increased with a smaller focal distance of the lens. Another way to optimize the measurement accuracy and therefore reduce the measuring range is to use an industrial vision lens. These vision lenses are corrected to have low chromatic aberration. First insights of a simulation have shown that an industrial vision lens can theoretically be used for such a measurement task. A possible future approach is to check whether such lenses are suitable for resolving smaller structures and obtaining depth information. This means to repeat the same procedure for different

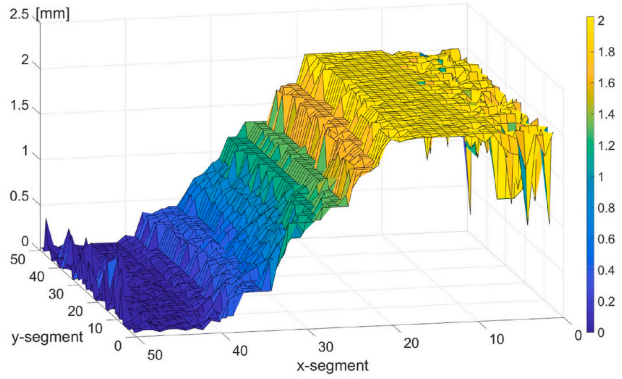

Fig. 5. 3D-map of test object (inclined plane).

Table 2
Comparison of experimental data and simulated/numerical data.

Wavelength in nm	Depth in mm	
	Experimental depth of inclined plane	Numeric/Simulated
500	0 (shifted)	0
520	0.636	0.487
540	1.116	0.928
560	1.696	1.328
580	2.014	1.692
600	2.120	2.025

vision lenses and examine to which extent they are capable for a high-resolution 3D depth measurement.

Acknowledgments

This research did not receive any specific grant from funding agencies in the public, commercial, or not-for-profit sectors.

References

[1] E. Hecht, Optics, Addison Wesley Longman, Inc., United States, 1998, p. 271.
[2] V.N. Mahajan, Optical Imaging and Aberrations - Ray Geometrical Optics, SPIE, Bellingham, Washington, 1998, pp. 25–26.
[3] Refractive Index of Schott N-Bk7, Schott Optical Glass Catalogue of August 2010, 2021. https://www.filmetrics.de/refractive-index-database/Schott+N-BK7/. (Accessed 24 February 2021).
[4] J.M. Tenenbaum, Accommodation in Computer Vision, PhD thesis, Stanford University, USA, 1970.

Robin Horn*
Technische Universität Ilmenau, Postfach 100565, 98684, Ilmenau, Germany

Maik Rosenberger
Technische Universität Ilmenau, Postfach 100565, 98684, Ilmenau, Germany
E-mail address: maik.rosenberger@tu-ilmenau.de.

Gunther Notni
Technische Universität Ilmenau, Postfach 100565, 98684, Ilmenau, Germany
E-mail address: gunther.notni@tu-ilmenau.de.

Andrei Golomoz
Technische Universität Ilmenau, Postfach 100565, 98684, Ilmenau, Germany
E-mail address: andrei.golomoz@tu-ilmenau.de.

Richard Fütterer
Technische Universität Ilmenau, Postfach 100565, 98684, Ilmenau, Germany
E-mail address: richard.fuetterer@tu-ilmenau.de.

Paul-Gerald Dittrich
Technische Universität Ilmenau, Postfach 100565, 98684, Ilmenau, Germany
E-mail address: paul-gerald.dittrich@tu-ilmenau.de.

* Corresponding author.
E-mail address: robin.horn@tu-ilmenau.de (R. Horn).